DESIGN AND TEST OF DOUBLE-SHAFT TYPE SWEET POTATO HAULM CUTTING RETURN MACHINE
/
双轴式甘薯打秧还田机设计与试验

Kuan QIN*), Yun ZHAO, Rui YANG
College of Engineering, Anhui Agricultural University, Anhui, Hefei, 230036 / China;
Tel: +86 18855102551; E-mail:qinkuan@ahau.edu.cn
DOI: https://doi.org/10.35633/inmateh-72-37

Keywords: *Design, Double-shaft type sweet potato haulm cutting return machine, Orthogonal test, Response surface*

ABSTRACT
In this study, a double-shaft type sweet potato haulm cutting return machine was designed. The structure of the whole machine as well as the key components were analyzed, and the influence of each factor on the operation quality was studied. The results of the study showed that the order of the influence of each factor on the length of broken stems and leaves and the rate of checking was as follows: roller speed > toggle ground clearance > toggle spacing; the order of the influence on the stubble height was as follows: toggle clearance > roller speed > toggle spacing; and the order of the influence on the rate of injury to potatoes was as follows: roller speed = toggle clearance = toggle spacing. The optimal combination of working parameters in the field test was 1944 r/min for roll speed, 132 mm for toggle spacing, and 20 mm for toggle clearance, at which the qualification rate of stem and leaf breaking length was 94.32%, stubble height was 33.61 mm, and potato injury rate was 0.26%. The relative error with the theoretical optimization value is between 0.13% and 7.14%, which meets the operational requirements of sweet potato rice transplanter.

摘要
本研究设计了双轴式甘薯打秧还田机。分析了整机结构以及关键部件，并研究了各因素对作业质量的影响。研究结果表明:各因素对茎叶打碎长度及格率的影响顺序为杆辊转速>拨杆离地间隙>拨杆间距，对留茬高度的影响顺序为拨杆离地间隙>杆辊转速>拨杆间距，对伤薯率的影响顺序为杆辊转速=拨杆离地间隙=拨杆间距。田间试验最优工作参数组合为杆辊转速 1944 r/min、拨杆间距 132 mm、拨杆离地间隙 20 mm，此时茎叶打碎长度合格率为 94.32%、留茬高度为 33.61 mm、伤薯率 0.26%。与理论优化值的相对误差在 0.13%~7.14%之间，满足甘薯打秧机的作业需求。

INTRODUCTION
Sweet potatoes belong to the sweet potato genus of the family Cyclophyllaceae and are also known as sweet potatoes, groundnuts, etc., which varies from place to place (*Gao et al., 2018*). Sweet potato contains a variety of beneficial substances for human health and high content of purple potato anthocyanins, with good health effects (*Lian et al., 2009*; *Wang et al., 2012; He et al., 2013; Hu et al., 2016; Xie et al., 2022*). China is the world's largest sweet potato producer (*Phesatcha et al., 2013; Yuan et al., 2016*). According to the statistics of the Food and Agriculture Organization of the United Nations (FAO), it can be seen that China's total sweet potato production in 2019 was 5.2×107 t, accounting for 56.62% of the total global sweet potato production (*Chen et al., 2022*).

Before harvesting sweet potatoes, haulm must be removed. Earlier haulm removal prevents the loss of sweet potato nutrients and reduces the rate of potato injury during harvest. However, sweet potato haulm have long vines and luxuriant growth, and the vines are too long and may even cover several sweet potato ridges, resulting in the entanglement of several sweet potato haulm. Manual haulm removal is time-consuming, labor-intensive and not economically efficient (*Xia et al., 2011*), and sweet potato haulm cutting machinery can improve productivity and reduce costs.

Kuan Qin, A.P. Ph.D. Eng.; Yun Zhao, M.S. Stud. Eng.; Rui Yang M.S. Stud. Eng.

The development of foreign sweet potato haulm and vine handling machinery started earlier, and its related technology is relatively mature, while having a high degree of automation (*Amer et al., 2012; Amer et al., 2013*). Sweet potato haulm cutting machinery can be divided into two main types: the first is a joint harvest, the haulm and vine crushing, digging sweet potato, potato and haulm separation, haulm and vine cleaning, harvesting and other aspects of a one-time completion. Relevant representative machines are: the United States Model 674 sweet potato direct harvesting combined harvesting machinery and the TSP series of towed sweet potato combined harvesting equipment produced by Standen Agricultural Machinery Company in the United Kingdom. The second is segmented harvesting, in which sweet potato haulm and vines are first crushed by haulm cutting machinery during digging and harvesting of sweet potato. Relevant representative machine: Germany Grimme (GRIMME) Company developed the KS75-4 type four rows of haulm cutting machine. Due to the foreign sweet potato planting model, resulting in the related machinery large size, power demand, agronomy and agro-mechanical requirements are strict (Wu et al., 2018), China has not yet been able to adopt the model, so it is difficult to promote it domestically. China's sweet potato haulm and vine handling machinery development is relatively lagging behind, in recent years the machinery is mostly based on potato rice transplanter and straw crushing machine developed. Relevant representative machines include the 4US-1 haulm cutting developed and manufactured by Tengzhou Golden Potato King, and the 4UL-80 potato haulm cutting developed and manufactured by Fuyang Agricultural Machinery Institute. Most of the domestic research and development of sweet potato haulm and vine processing machinery is only crushing shaft of the one shaft haulm cutting machine, a number of problems such as poorly qualified stem and leaf breaking lengths and high stubble heights were prevalent.

In this paper, for the current domestic one shaft haulm cutting machine existing general problems, combined with sweet potato planting mode and physical characteristics of haulm, a double-shaft type sweet potato haulm cutting machine was researched and designed.

MATERIALS AND METHODS

Structure and working principle of the whole machine

Double-shaft type sweet potato haulm cutting return machine is mainly composed of flail knife, transmission system, haulm picking device, haulm cutting device and other components. The basic structure is shown in Figure 1.

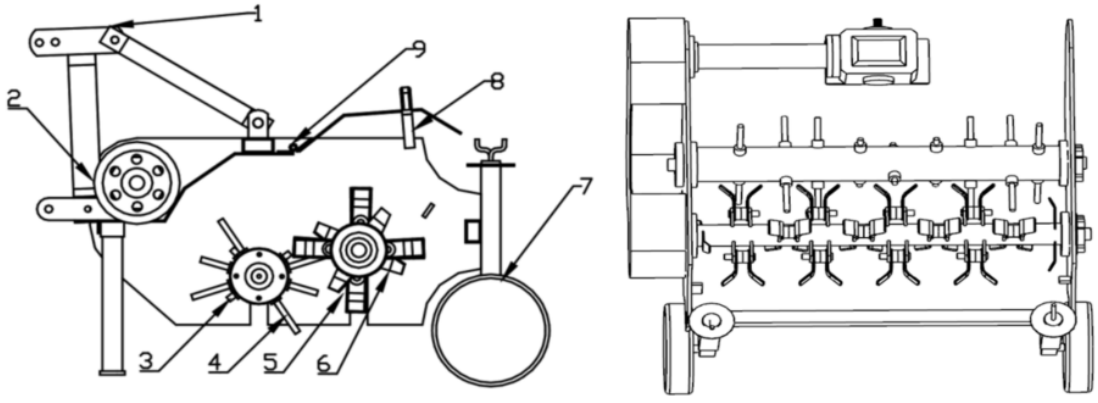

Fig. 1 - Schematic diagram of the structure of double-shaft type sweet potato haulm cutting return machine

1-suspension frame; 2-gear box; 3-haulm picking device; 4-toggle lever; 5-haulm cutting device; 6-flail knife; 7-depth limiting wheel; 8-row of fixed knife device; 9-cover of the whole machine.

When the double shaft type sweet potato haulm cutting return machine works, the power generated by its traction tractor engine is input to the gearbox through the transmission shaft, and then the power is transmitted to the main pulley through the gear shaft. The main belt pulley then conveys the power to the haulm picking device belt pulley and the haulm cutting device belt pulley respectively, and the haulm picking device belt pulley drives the rod shaft to rotate at a high speed, and picks up the haulm stalks creeping on the surface of the sweet potato ridge and throws them backward and upward. Once the upper haulm cutting device with the flail knife cuts and crushes the sweet potato vines and haulm, simultaneously, a row of fixed knives on the cover shell wall performs secondary crushing on the already crushed haulm and vine. Ultimately, the crushed haulm and vine stalks are thrown in a high-speed manner, sliding uniformly along the cover shell wall to the surface of the ridge. The structural and operating parameters of the machine are shown in Table 1.

Table 1

Structural parameters of the double-shaft type potato haulm cutting return machine

Serial number	Project name	Unit	Design specification
01	Overall dimensions (L*W*H)	mm	1200*1300*800
02	Auxiliary power	kw	36.8
03	Working width	mm	900
04	Number of rows	line	1
05	Traveling speed	km/h	5~10
06	Rotation speed of haulm picking device	r/min	≥1500
07	Rotation speed of seeding device	r/min	≥1500
08	Pure hourly production efficiency	hm^2/h	1±0.2
09	Overall quality	kg	220±10

Design and calculation of key components

Design of haulm picking device

Double-shaft type potato haulm cutting return machine compared to the traditional one shaft sweet potato haulm cutting machine increased picking device, the device reduces the power of the knife in the haulm cutting device, reduces the rate of injury to the potato and solves the traditional one-shaft haulm cutting machinery field operation when the vines entangled the equipment. The haulm picking device is mainly composed of rod roller shaft, rod holder, toggle rod and other components, as shown in Figure 2.

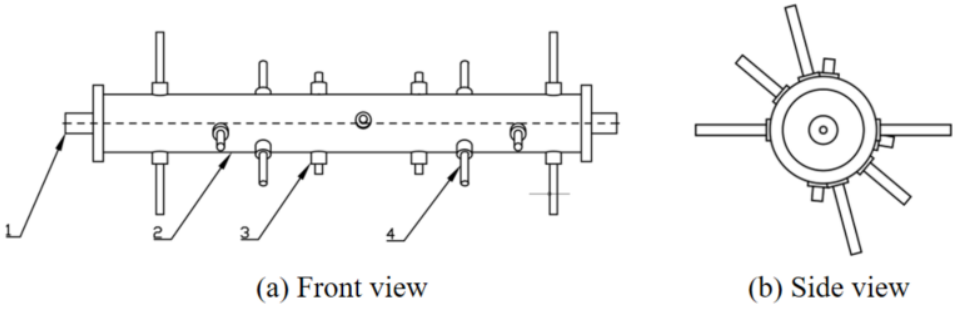

Fig. 2 - Structure of haulm picking device

1 - shaft head; 2 - rod roller shaft; 3 - rod holder; 4 - toggle rod.

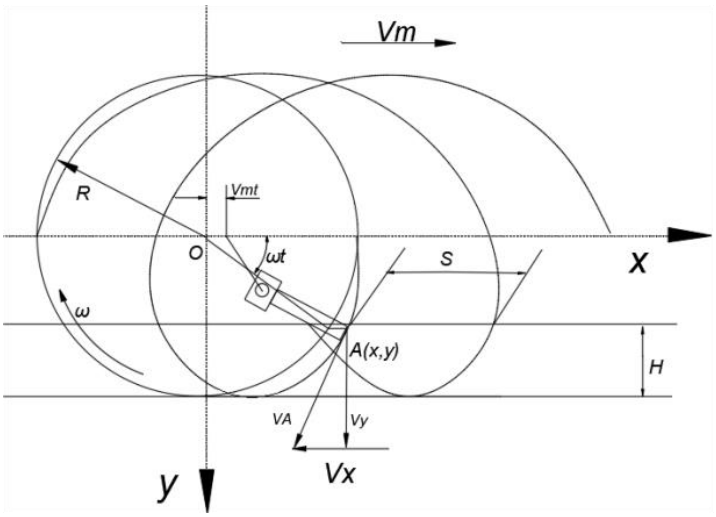

Fig. 3 - Toggle rod movement trajectory diagram

The toggle rod is the key component of the haulm picking device, and its shape, material, quantity and arrangement will affect the haulm cutting effect after operation. After a number of prototype tests, in order to pick up the haulm and not to cut the stalks of the haulm to affect the efficiency of the subsequent haulm cutting stage, the toggle rod adopts a cylinder with a diameter of 15 mm, and the material chosen is 65 Mn steel sheet, the hardness of which can reach 48~56 HRC after heat treatment. The number of toggle rods is 18 and the arrangement is a double helix arrangement structure (*Zhang et al., 2007*).

The rotation speed of the rod roller of the toggle rod is one of the main parameters of the haulm picking device. When the machine is in operation, the toggle rod produces both linear and circular motions at the same time, and the absolute motion of the toggle rod is synthesized from the above two motions. It can be concluded that the trajectory of any point on the toggle rod is a regular curve, i.e., a pendulum. When the radius of motion of the toggle rod is R, the forward speed of the whole machine is v_m, and the angular velocity of the rotation is ω, the coordinate system O point is used as the origin coordinate system, as shown in Fig. 3.

The initial rotation center of the toggle rod shaft is set as the origin of the coordinate system, the forward direction of the haulm cutting machine is set as the x-axis, the direction perpendicular to the downward direction of the forward direction is set as the y-axis, and the radius of rotation of the toggle rod movement is R. The relationship between the time t and the coordinates of the toggle rod tip is shown in Equation 1:

$$\begin{cases} x = R\cos\omega t + v_m t \\ y = R\sin\omega t \end{cases} \quad (1)$$

where: v_m is the forward speed of the whole machine, [m/s]; R is the radius of the toggle rod roll circumference, [m].

The expression for the velocity of motion at the endpoint of the toggle rod is Equation 2:

$$\begin{cases} v_x = \dfrac{d_x}{d_t} = v_m - R\cdot\omega\cdot\sin\omega t \\ v_y = \dfrac{d_y}{d_t} = R\cdot\omega\cdot\cos\omega t \end{cases} \quad (2)$$

where: v_x is the horizontal partial velocity at the endpoint of the toggle rod, [m/s]; v_y is the vertical partial velocity at which the toggle rod is disconnected, [m/s].

The expression for the absolute velocity of motion at the endpoint of the toggle rod is Equation 3:

$$v = \sqrt{v_x^2 + v_y^2} = \sqrt{v_m^2 + R^2\omega^2 - 2v_m R\omega\sin\omega t} \quad (3)$$

The circular velocity of the end point of the toggle rod $v_p = R\omega$, so that $\lambda = v_p/v_m = R\omega/v_m$, where λ is the rotational speed ratio, and the size of the λ value has a direct impact on the trajectory of the toggle rod and the operational efficiency. Therefore, substituting $\lambda = R\omega/v_m$ into Equation 2 leads to Equation 4:

$$v_x = v_m - R\cdot\omega\cdot\sin\omega t = v_m(1 - \lambda\cdot\sin\omega t) \quad (4)$$

When λ < 1, there must be v_x>0 regardless of any position of the toggle rod motion. That is, the horizontal partial velocity of the end point of the toggle rod is always the same as the forward direction of the whole haulm cutting machine, and its trajectory is a pendulum line, at which time the toggle rod throws backward sweet potato haulm and vines. When λ>1, the toggle rod moves to a certain position, v_x<0, i.e., the horizontal partial velocity at the end point of the toggle rod is opposite to the forward direction of the whole machine, and its trajectory is a trochoid. The machine works properly when the trajectory of any point of the toggle rod endpoint is a trochoid. The design study of the double-shaft type sweet potato haulm cutting return machine takes λ>1. Therefore, to ensure that v_x<0, at this time $\sin\omega = (R-H)/R$, which leads to Equation 5:

$$n \geq 30(v_c + v_m)/[\pi(R - H)] \quad (5)$$

where: v_c is the picking speed of the toggle rod, [m/s]; n is the rotational speed of the toggle rod, [r/min]; H is the picked haulm thickness, [m].

When picking haulm, v_m = 0.55m/s, v_c = 23m/s, H = 0.15m, R = 0.303m (the maximum radius of rotation of the toggle rod lever) is substituted into Equation 5, and n≥1469 can be obtained, so the rotation speed of the toggle rod lever roller should be not less than 1469 r/min.

Design of haulm cutting device

The haulm cutting device is the key component of the double-shaft type sweet potato haulm cutting return machine, which mainly destroys and crushes the haulm vines thrown by the picking device when the machine is in operation. The haulm cutting device mainly consists of a flail knife, a knife holder, a knife roller shaft, and pin shaft, as shown in Fig. 4. In order to minimize the weight of the whole machine and thus reduce energy consumption, the knife roller shaft adopts a hollow shaft (*Du et al., 2015*).

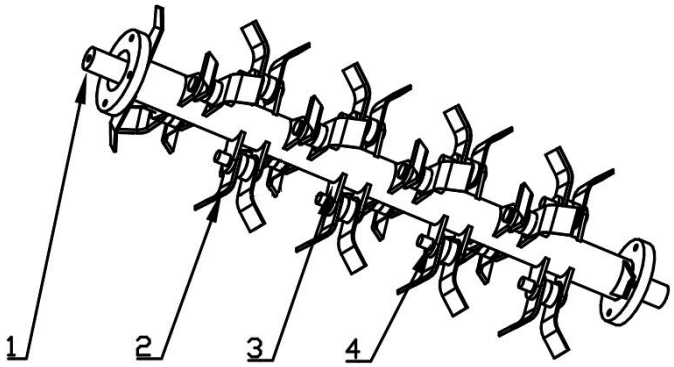

Fig. 4 - Structure of seeding device

1-shaft head; 2-flail knife; 3-knife holder; 4-knife roller shaft.

As a key component of the haulm cutting device of the double-shaft type sweet potato haulm cutting return machine, the flail knife plays a very important role in the operation of the machine. At present, the Y-type flail knife is the most widely used knife type, with strong shear force, double-sided open edge, and high qualified rate of stem and leaf breaking. In this study, an improved Y-type flail knife was designed as shown in Fig. 5. Since the flail knife is a wear part, 65 Mn steel sheet was chosen for its material (*Li et al., 2014*). After heat treatment, the hardness of the knife reaches 48~56 HRC and the hardness of the shank reaches 33~40 HRC.

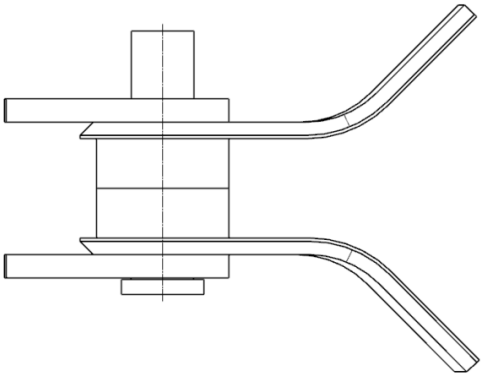

Fig. 5 - Schematic diagram of the improved Y-type flail knife

The number and arrangement of flail knives have a great impact on the machine's operating performance. The design of the number of flail knives should be reasonable, if the number is too small, the leakage rate increases, and the operation effect is unqualified. If the number is too big, it is easy to produce clogging phenomenon during operation, and the power consumed will increase (*Pan et al., 2015*).

Equation 6 can be used to calculate the number of flail knives:

$$N_1 = C_1 \times L_1 \tag{6}$$

where:

N_1 is the total number of knives, [roots]; C_1 is the density of knives, [roots/mm]; L_1 is the working width of the machine, [mm].

The density of the Y-shaped flail knife was taken as 0.02-0.04 pieces/mm (*Gu et al., 2016*). In designing the double-shaft type sweet potato haulm cutting machine, the operating width of the machine was designed to be 900 mm, i.e., L_1 was 900 mm. Substituting the data obtained above into Equation 6, it can be obtained that the number of improved Y-type flail knives should be 16 by removing the L-type flail knives at both ends of the four-piece knife roller shaft.

In order to ensure the stability of the machine during operation and the uniform loading of the knife rollers, the axial distance between the flail knives should be as large as possible to avoid clogging (*Lv et al., 2016*). To synthesize the advantages and disadvantages of various arrangements, the machine adopts a staggered and balanced arrangement, as shown in Figure 6.

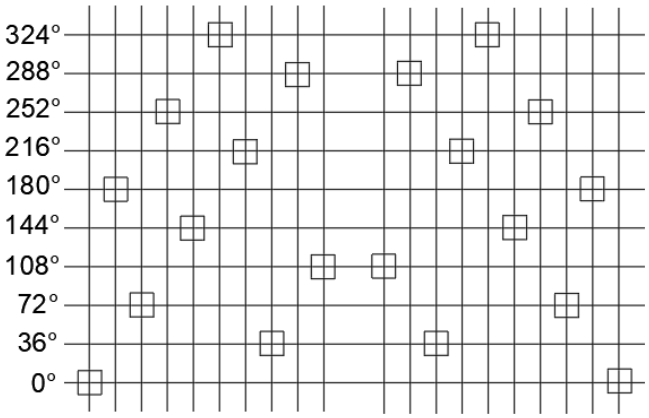

Fig. 6 - Schematic diagram of the improved Y-type flail knife

The cutter shaft is usually considered to be a homogeneous rotating body, i.e. the centrifugal force of the cutter shaft is close to zero. The vibrations to which the machine is subjected during operation come from the centrifugal force generated by the high speed rotation of the knife rollers and transmitted through the bearings. The centrifugal force generated by the knife and attachments is the cause of the moment on the pivot point of the knife roll and the cause of vibration. If the degree of vibration of the whole machine is to be minimized, the moment generated by the centrifugal force of the flail knife on the pivot point should be reduced to zero (*Li et al., 2020*). The centrifugal force of the knife roller shaft is analyzed as shown in Fig. 7.

From Fig. 7, the plane of symmetry of the first leftmost flail knife position is set as a, and the plane of symmetry of the first rightmost flail knife positionis set as b. According to the equilibrium equations (*Ji et al., 2003; Mu, 2021*), all the centrifugal forces are decomposed to the x,y-axis, and Equations 7 and 8 are obtained:

$$\begin{cases} F_{ax} = \sum_{N-1}^{N} \frac{N-i}{N-1} F\cos\theta \\ F_{ay} = \sum_{N-1}^{N} \frac{N-i}{N-1} F\sin\theta \end{cases} \tag{7}$$

$$\begin{cases} F_{bx} = \sum_{N-1}^{N} \frac{N-i}{N-1} F\cos\theta \\ F_{by} = \sum_{N-1}^{N} \frac{N-i}{N-1} F\sin\theta \end{cases} \tag{8}$$

where:

F is the centrifugal force on the flail knives and their holders, [N]; N is the number of flail knives, [pieces]; i is the order of the flail knives; and θ is the angle between adjacent flail knives, [°].

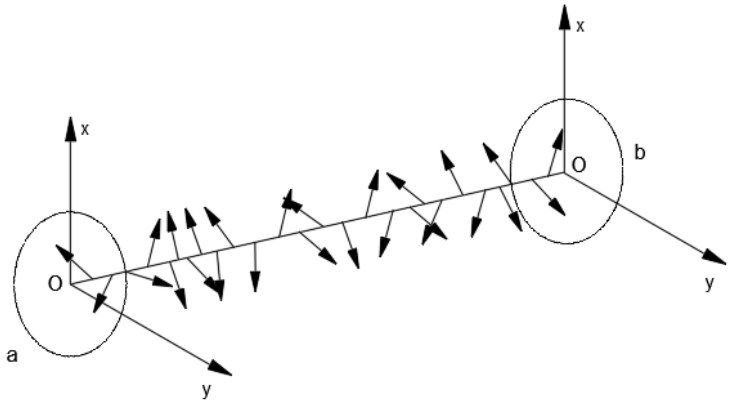

Fig. 7 - Knife roller shaft centrifugal force analysis diagram

The values obtained for the knife arrangement are substituted into Equations 7 and 8 for calibration calculations, and the results obtained show that the number and arrangement of knife designs are reasonable.

Drive train design

The traction power was selected from a Changchai 4L68 diesel tractor with a power output speed n1 of 1200 r/min. A schematic diagram of the drive train is shown in Figure 8.

With the known diameter and number of teeth of the gearbox gears, the total transmission ratio of the haulm cutting machine can be calculated, Equation 9:

$$i = \frac{z_1}{z_2} \times \frac{p_1}{p_2} = 1.87 \quad (9)$$

where: z_1, z_2 is the number of teeth of the gearbox gear, [pcs]; p_1, p_2 is the diameter of the gearbox gear, [mm].

Substituting the known tractor power output speed n_1=1200 r/min and the total transmission ratio of the haulm cutting machine. i =1.87 into Equation 9, it can be concluded that the rotational speed of rod roller and knife roller of the double-shaft type sweet potato haulm cutting return machine n_{max}=2244 r/min, which is in line with the operational requirements of the haulm cutting machine.

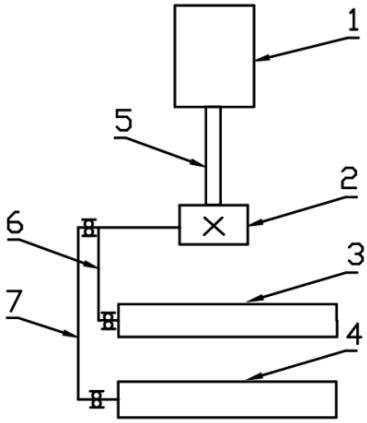

Fig. 8 - Schematic diagram of transmission system of double shaft type sweet potato haulm cutting return machine

1-engine; 2-gearbox; 3-haulm picking device; 4-haulm cutting device; 5-drive shaft; 6-pulley 1; 7-pulley 2

Parameter optimization test

The location of this experiment was in the sweet potato planting base in Dailukou Township, Si County, Suzhou City, Anhui Province, where the local soil type is sandy loam. The average water content was 16.2%, and the soil had good air and water permeability and loose texture, which was suitable for sweet potato cultivation. The average width of the rows was 900 mm and the average spacing of the rows was 200 mm. The sweet potatoes were harvested at the time of the experiment, and the stalks of the sweet potato haulm were 150 mm from the roots and about 60 mm in length.

The test equipment and instruments mainly include: 4L68 diesel tractor, double-shaft type sweet potato haulm cutting return machine, moisture meter, tape measure, electronic balance, stopwatch, tachometer, marker, scissors and so on.

The experiments were conducted to determine the length and percentage of broken stems and leaves Z_1, the average stubble height Z_2, and the injury rate Z_3 of the double-shaft type sweet potato haulm cutting return machine under different working parameters as their evaluation indexes. There are many factors affecting the evaluation indexes of the twin-axle sweet potato rice-planting and field-returning machine, and it was determined on the basis of the previous test that the rod roller speed A (the same speed of the rod roller and the knife roller), the toggle rod spacing B, and the toggle rod clearance C were taken as the main factors affecting the operational performance, and the test factors and levels were shown in Table 2.

Before operation, 2 round trips were measured, and 5 equally spaced 1 m square performance measurement points were selected within each trip, as shown in Figure 9. All broken stalks within each performance measurement point were collected and weighed, and then stalks with a length greater than 100 mm were singled out from them and weighed, and the length of broken stalks within each performance measurement point and the pass rate were calculated according to Equation 10, and the average of 10 measurement points in 2 round-trip journeys was randomly selected.

$$Z_1 = \frac{m_y - m_b}{m_y} \times 100 \quad (10)$$

where:

Z_1 is the pass rate for broken stem length, [%]; m_b is the mass of broken stems, [kg]; m_y is the mass of broken stems >100 mm, [kg].

Table 2

Test factors and level

Level	Factor		
	Rod roller speed A / (r/min)	Toggle rod spacing B / (mm)	Toggle rod ground clearance C / (mm)
1	2200	150	25
0	1850	125	20
-1	1500	100	15

Fig. 9 - Performance test sample point

The length of 10 stubble stubs was randomly selected at the performance measurement points after the seeding operation, and the average of the 10 measurement points in 2 round trip trips was randomly selected.

$$Z_2 = \frac{L_N}{N} \quad (11)$$

where:

Z_2 is the average stubble height on the ridge, [mm]; L_N is the sum of stubble heights, [mm]; N is the number of plants measured, [n].

All sweet potatoes in the area of each measurement point were dug out and weighed, and then the wounded potatoes among them were picked out and weighed, and the rate of wounded potatoes within each measurement point was calculated according to Equation 12, and the average of the 10 measurement points in the 2 round-trip journeys was randomly selected.

$$Z_3 = \frac{M_s}{M} \times 100 \quad (12)$$

where:

Z_3 is the rate of injury, [%]; M_s is the mass of injured potatoes, [kg].; M is the total mass of sweet potatoes in each performance point, [kg].

RESULTS

Test results

Box-Behnken principle was used to design a three-factor, three-level quadratic regression orthogonal test (*Zhang et al., 2015*), and the test protocol and response values are shown in Table 3.

Table 3

Test scheme and results

Test serial number	Level of factors			Response value		
	A	B	C	Z_1	Z_2	Z_3
1	2200	125	25	90.35	58	0.3
2	1500	125	25	61.87	84	0.02
3	1850	150	15	86.61	48	0.42
4	1500	125	15	85.06	50	0.47
5	2200	100	20	81.04	42	0.55
6	1850	150	25	75.07	63	0.05
7	1850	125	20	94.45	30	0.24
8	1850	100	15	82.43	40	0.49
9	2200	125	15	98.49	18	0.57
10	1500	150	20	65.44	69	0.11
11	1850	125	20	92.93	34	0.22
12	1850	125	20	90.06	35	0.25
13	1850	125	20	94.16	39	0.22
14	1500	100	20	65.82	64	0.3
15	2200	150	20	87.95	40	0.31
16	1850	125	20	92.98	31	0.26
17	1850	100	25	76.64	66	0.32

Regression modeling and significance test analysis

Combining the experimental and resultant data obtained from Table 3, the results obtained from this experiment were analytically optimized and fitted with multiple regression using Design-Expert 11.0 analysis software (*Shi et al., 2017; Wu et al., 2017*). A quadratic polynomial response surface regression model was developed for Z_1, Z_2, and Z_3 on the three independent variables A, B, and C.

After analyzing the data with Design-Expert software, the regression equations for Z_1, Z_2, Z_3 were fitted as shown in Equation 13.

$$\begin{cases} Z_1 = 92.92 + 9.96A - 6.08B + 1.14C + 3.76AB + 1.82AC - \\ 1.44BC - 7.05A^2 - 1.92B^2 - 10.80C^2 \\ Z_2 = 33.80 - 13.62A + 14.38B + 1.00C + 1.50AB - 1.75AC - \\ 2.75BC + 9.10A^2 + 9.60B^2 + 10.85C^2 \\ Z_3 = 0.2380 + 0.1037A - 0.1575B - 0.0963C + 0.0450AB - \\ 0.0125AC - 0.050BC + 0.0498A^2 + 0.0522B^2 + 0.0298C^2 \end{cases} \quad (13)$$

Table 4

Analysis of variance of Z_1 regression equation for stem and leaf fragmentation length

Source of variation	Z_1				
	Square sum	Degrees of freedom	Mean square	*F-value*	*P-value*
Model	1949.95	9	216.66	37.29	< 0.0001
A	792.82	1	792.82	136.47	< 0.0001
B	10.44	1	10.44	1.80	0.2219
C	295.97	1	295.97	50.95	0.0002
AB	56.63	1	56.63	9.75	0.0168
AC	13.29	1	13.29	2.29	0.1742
BC	8.27	1	8.27	1.42	0.2718
A^2	209.23	1	209.23	36.01	0.0005
B^2	15.59	1	15.59	2.68	0.1454
C^2	491.50	1	491.50	84.60	< 0.0001
Residual	40.67	7	5.81		
Incoherent	28.60	3	9.53	3.16	0.1476
Inaccuracies	12.06	4	3.02		
Aggregate	1990.62	16			

As can be seen from Table 4, the four regression terms A, B, A^2, and C^2 had extremely significant effects on Z_1 ($P < 0.01$). AB had a more significant effect on Z_1 ($0.01 < P < 0.05$).C, AC, BC, and B^2 did not have a significant effect on Z_1 ($P > 0.1$). Since the value of misfit P = 0.1476 is greater than 0.05, the model does not have to take into account any interaction term between the factors, i.e., the effect of the other factors on the length of stem and leaf breaking is not significant. Some of the factors whose effects were not significant were removed and then their models were optimized to arrive at the regression Equation 14 (*Yan et al., 2017*).

$$Z_1 = 92.92 + 9.96A - 6.08B + 3.76AB - 7.05A^2 - 10.80C^2 \quad (14)$$

As can be seen from Table 5, A, B, A^2, B^2, and C^2 were extremely significant ($P < 0.01$) on Z_2. C, AB, AC, and BC were not significant ($P > 0.1$) on Z_2. Since the value of misfit P = 0.1172 is greater than 0.05, the model does not have to take into account any interaction term between the factors, i.e., the effect of other factors on stubble height is not significant. Some of the factors with insignificant effects were removed and then their models were optimized to obtain regression equation 15.

$$Z_2 = 33.80 - 13.62A + 14.38B + 9.10A^2 + 9.60B^2 + 10.85C^2 \quad (15)$$

Table 5

Analysis of variance of the Z2 regression equation for stubble retention height

Source of variation	Z_2				
	Square sum	**Degrees of freedom**	**Mean square**	***F-value***	***P-value***
Model	4573.98	9	508.22	18.38	0.0004
A	1485.12	1	1485.12	53.71	0.0002
B	8.00	1	8.00	0.2893	0.6073
C	1653.13	1	1653.13	59.79	0.0001
AB	9.00	1	9.00	0.3255	0.5862
AC	12.25	1	12.25	0.4430	0.5270
BC	30.25	1	30.25	1.09	0.3303
A^2	348.67	1	348.67	12.61	0.0093
B^2	388.04	1	388.04	14.03	0.0072
C^2	495.67	1	495.67	17.93	0.0039
Residual	193.55	7	27.65		
Incoherent	142.75	3	47.58	3.75	0.1172
Inaccuracies	50.80	4	12.70		
Aggregate	4767.53	16			

As can be seen from Table 6, A, B, and C had extremely significant effects on Z_3 ($P < 0.01$). AB, BC, A^2, and B^2 had more significant effects on Z_3 ($0.01 < P$ less than 0.05).C^2 had significant effects on Z_3 ($0.05 < P < 0.1$). AC had no significant effect on Z_3 ($P > 0.1$). Since the value of misfit P = 0.0595 is greater than 0.05, the model does not have to take into account any interaction term between the factors, i.e., the effect of other factors on stubble height is not significant. Some of the factors with insignificant effects were removed and then their models were optimized to obtain regression equation 16.

$$Z_3 = 0.2380 + 0.1037A - 0.1575B - 0.0963C + 0.0450AB - 0.050BC + 0.0498A^2 + 0.0522B^2 + 0.0298C^2 \quad (16)$$

Table 6

Analysis of variance in the Z3 regression equation for the rate of wounded potatoes

Source of variation	Z_3				
	Square sum	**Degrees of freedom**	**Mean square**	***F-value***	***P-value***
Model	0.4058	9	0.0451	45.39	< 0.0001
A	0.0861	1	0.0861	86.67	< 0.0001
B	0.0741	1	0.0741	74.59	< 0.0001
C	0.1984	1	0.1984	199.73	< 0.0001
AB	0.0081	1	0.0081	8.15	0.0245
AC	0.0006	1	0.0006	0.6290	0.4537
BC	0.0100	1	0.0100	10.06	0.0157
A^2	0.0104	1	0.0104	10.49	0.0143
B^2	0.0115	1	0.0115	11.57	0.0114
C^2	0.0037	1	0.0037	3.75	0.0940
Residual	0.0070	7	0.0010		
Incoherent	0.0057	3	0.0019	5.91	0.0595
Inaccuracies	0.0013	4	0.0003		
Aggregate	0.4128	16			

As shown in Tables 4, 5, and 6, the P-values of the response surface models for stem and leaf breaking length and qualification rate Z1, stubble height Z2, and potato injury rate Z3 were less than 0.01, indicating that the regression models were extremely significant (*Yu et al., 2015*). The P-values of the misfit terms were 0.1476, 0.1172, and 0.0595 were all greater than 0.05, indicating that the regression equation was highly fitted.

Response surface analysis

With the results obtained above, the response surface was plotted for the model using Design-expert 11.0 software, and the effects of the interaction terms between factors A, B, and C on Z_1, Z_2, and Z_3, respectively, were analyzed based on the response surface.

The interaction terms with more significant effect on Z_1 were selected for response surface analysis. Table 4 shows that the factor interaction term with the smallest p-value is AB and therefore has a more significant effect on Z_1. When B is 125 mm, the response surface is shown in Fig. 10. It can be seen that when A is fixed, Z_1 increases and then decreases with the increase of C. The optimal C is between 19 and 21 mm. When C was fixed, Z_1 first increased and then decreased with increasing A. The optimal A was between 1800 and 1900 r/min. In the interaction between both A and C, the magnitude of A is the main factor affecting the length of stem and leaf breaking and Z_1 (Zhao et al., 2018).

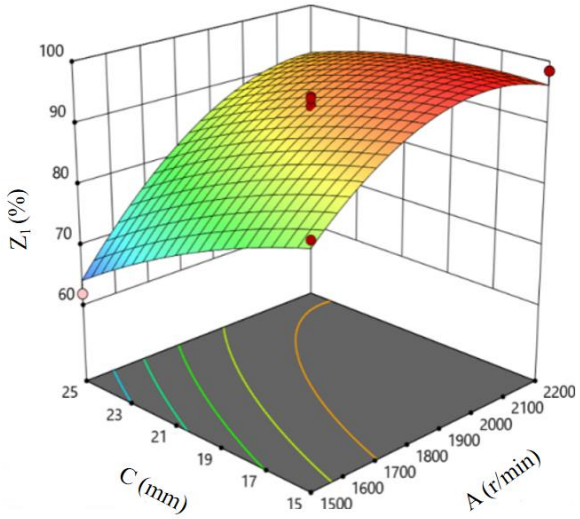

Fig. 10 - Interaction of rod-roller speed and toggle rod clearance C=125 mm

The interaction terms with more significant effects on Z_2 were selected for response surface analysis. Table 5 shows that the factor interaction term with the smallest p-value is the interaction term BC between C and B. Therefore, the effect on Z_2 is more significant. When A is 1850 r/min, the response surface is shown in Fig. 11. It can be seen that when B is fixed, Z_2 increases as C increases and the optimum C is between 19 and 21 mm. When C is fixed, Z_2 decreases and then increases with increasing B. The optimal B is between 120 and 130 mm. In the interaction between C and B, the size of B is the main factor affecting Z_2.

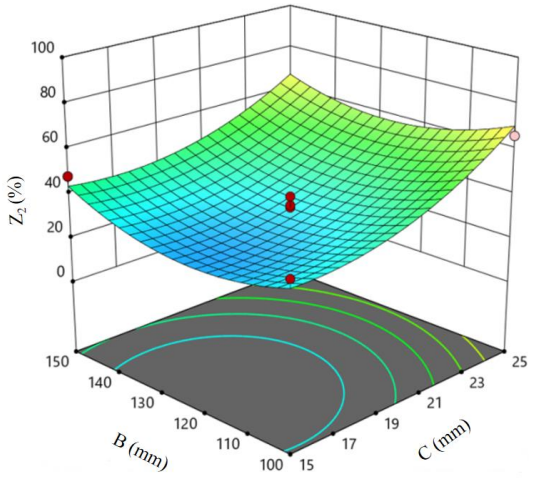

Fig. 11 - Interaction of toggle rod spacing and toggle rod ground clearance A = 1850 r/min

The interaction terms with more significant effects on Z_3 were selected for response surface analysis. As can be seen from Table 6, the interaction term BC of C and B, which has the smallest p-value among the factor interaction terms, therefore has a more significant effect on Z_3. When A is 1850 r/min, the response surface is shown in Fig. 12. It can be seen that when C is fixed, Z_3 decreases as B increases and the optimal B is between 120 and 130 mm. When B is fixed, Z_3 decreases and then increases with the increase of C, and the optimal C is between 19~21 mm. In the interaction between C and B, the size of C is the main factor affecting Z_3.

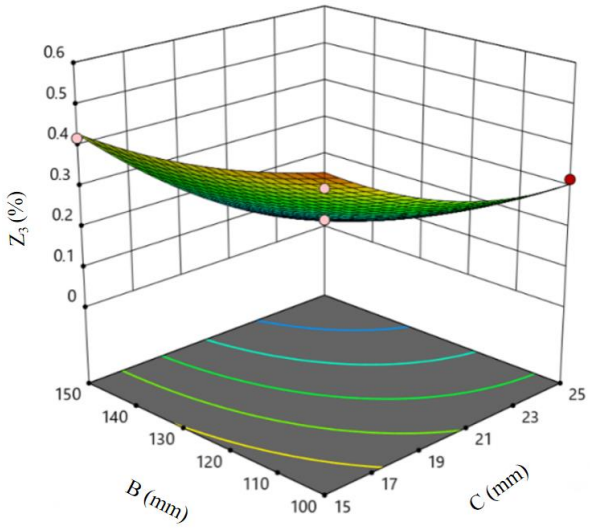

Fig. 12 - Interaction of toggle rod spacing and toggle rod ground clearance A = 1850 r/min

Parameter optimization and experimental validation

Through the analysis of the above three response surfaces, the regression models of Z_1, Z_2 and Z_3 were optimized and solved using the optimization module in the Design-Expert11.0 analysis software, and the optimization constraints were finally determined according to the actual operating conditions of rice-planting machine and the relevant group standards of rice-planting machinery class to meet the operating requirements of high pass rate of stem and leaf breaking length, low stubble height and low rate of injury to potatoes, as in Equation 17.

$$\begin{cases} \max Z_1(A,B,C) \\ \min Z_2(A,B,C) \\ \min Z_3(A,B,C) \\ A、B、C>0 \\ -1 \leqslant Z_f \leqslant 1 \end{cases} \quad (17)$$

(a) Before operation (b) After operation

Fig. 13 - Comparison of the effect of haulm cutting machine before and after field operation

The optimization solution using Design-Expert 11.0 analysis software yields optimal results of 94.45% for Z_1, 32.44 mm for Z_2 and 0.28% for Z_3 when A is 1943.87 r/min, B is 131.85 mm and C is 20.24 mm.

To further validate the optimization results, a field validation test was carried out using a double-shaft type sweet potato haulm cutting return machine at the sweet potato planting base in Dailukou Township, Siachen County, Anhui Province, as shown in Fig. 13. The rice-planting machines A, B, and C were set at 1944 r/min, 132 mm, and 20 mm, respectively, and the average values of 10 measurement points were randomly selected for 2 round trips. At this time, Z_1 is 94.32%, Z_2 is 33.61 mm, and Z_3 is 0.26%. As shown in Table 7, it can be concluded that the results of the comparison experiments are consistent with the results of the optimal parameter combinations derived from theoretical analysis, and also satisfy the industry standard of the double-shaft type sweet potato haulm cutting return machine.

Table 7

Theoretical analysis results, comparative test results and reference indicators are compared

Serial number	Z_1	Z_2	Z_3
Optimizing the average	94.45	32.44	0.28
Test Mean	94.32	33.61	0.26
Relative error/%	0.13	2.03	7.14

CONCLUSIONS

(1) The main influencing factors for the test of a double-shaft type sweet potato haulm cutting return machine were analyzed and determined: rod-roller speed, toggle rod clearance from the ground, and toggle rod spacing. The three-factor, three-level quadratic regression orthogonal test was designed using Box-Behnken principle with stem and leaf breaking length and qualification rate, stubble height, and potato injury rate as test indexes, respectively. The effects of rod roller rotational speed, toggle rod spacing, and toggle ground clearance from the ground on the length of stem and leaf breaking, stubble height, and potato injury rate were analyzed and parameter optimization was carried out. The relative errors between the actual measured values and the theoretical optimized values were obtained between 0.13% and 7.14% through the validation test, which indicated that the model was highly reliable.

(2) The order of the effect of each factor on the length of broken stems and leaves and the rate of grams is the speed of the rod roller > toggle rod clearance > toggle rod spacing. The order of influence of each factor on stubble height is toggle ground clearance>roller speed>toggle rod spacing. The order of the influence of each factor on the rate of potato injury is roller speed = toggle rod clearance = toggle rod spacing.

(3) The optimal working parameters of the double-shaft type sweet potato haulm cutting return machine were 1944 r/min for the rotational speed of the rod rollers, 132 mm for the spacing of the toggle rod bars, and 20 mm for the clearance of the toggle rod bars from the ground, and at this time, the qualification rate of the length of the broken stems and leaves was 94.32%, and the stubble height was 33.61 mm, and the rate of injury to the potatoes was 0.26%.

ACKNOWLEDGEMENT

This work was supported by the National Natural Science Foundation of China (Grant No. 52105239), the Anhui Provincial Agricultural Material Technology Equipment Field Project (S202320230906020015) for the Development and Application of Yam Planting Machines (Line Type Automatic Yam Transplanter), and the Suzhou City Science and Technology Plan Project (SZKJXM202209) for the Key Technology Research and Equipment Development of Mechanized Production of Sweet Potatoes.

REFERENCES

[1] Amer, N., Kakahy, D., Ahmad, M. et al. (2012). Design and development of an Integrated Slasher (Pulverizer) for Sweet Potato Harvester: A Review. *IOP Conference Series: Materials Science and Engineering* (1). https://doi.org/10.1088/1757-899X/36/1/012007.

[2] Amer, N., Kakahy, D., Ahmad, M. et al. (2013). Effects of Knife Shapes and Cutting Speeds of a Mower on the Percentage Pulverization of Sweet Potato Vine. *Applied Mechanics and Materials* (421-421). https://doi.org/10.4028/www.scientific.net/AMM.421.29.

[3] Chen, X., Lu, J., Wang, X. et al. (2022). Analysis of Changes in Production Layout and Drivers of Sweet Potato in China (中国甘薯生产布局变迁及动因分析). *Chinese Journal of Agricultural Resources and Regional Planning,* 43(02):1-12. https://doi.org/10.7621/cjarrp.1005-9121.20220201.

[4] Du, H., (2015). Development of Sweet Potato Rice Stem Crushing and Returning Machine (红薯秧茎破碎还田机的研制). *Research on agricultural mechanization*, 37(11):113-116. https://doi.org/10.13427/j.cnki.njyi.2015.11.025.

[5] Gao, H., Sun, S., Chen, Y. et al. (2018). Theory and practice of sustainable development of sweet potato industry (甘薯产业可持续发展的理论与实践). *Journal of Hebei Normal University of Science&Technology*, (03), 65-70. https://doi.org/10.3969/J.ISSN.1672-7983.2018.03.012.

[6] Gu, F., Hu, Z., Chen, Y., et al. (2016). Development and experiment of peanut no-till planter under full wheat straw mulching based on “clean area planting” (“洁区播种”思路下麦茬全秸秆覆盖地花生免耕播种机研制). *Transactions of the Chinese Society of Agricultural Engineering*, 32(20):15-23. https://doi.org/10.11975/j.issn.1002-6819.2016.20.002.

[7] He, J., Cheng, L., Hong, Y., et al. (2013). Optimization of compound color fixative without sulfur during sweet potato flour processing (甘薯全粉加工中无硫复合护色工艺优化). *Transactions of the Chinese Society of Agricultural Engineering*, 29(9): 275-284. https://doi.org/10.3969/j.issn.1002-6819.2013.09.035.

[8] Hu, L., Wang, B., Wang, G., et al. (2016). Design and experiment of type 2ZGF-2 duplex sweet potato transplanter (2ZGF-2 型甘薯复式栽植机的设计与试验). *Transactions of the Chinese Society of Agricultural Engineering*, 32(10):8-16. https://doi.org/10.11975/j.issn.1002-6819.2016.10.002.

[9] Ji, J., Li, Q., Cai, Wei., (2003). Analysis of the effect of tool arrangement on the vibration of a stalk chopping and returning machine (刀具布置对茎秆切碎还田机振动的影响分析). *Research on agricultural mechanization*, (04):63-64. https://doi.org/10.13427/j.cnki.njyi.2003.04.025.

[10] Li, G., Li, Y., Zhang, X. et al. (2014). Design of the flail knife for the straw chopper and returning machine. (秸秆粉碎还田机甩刀的设计). *Research on agricultural mechanization*, 36(08):122-125. https://doi.org/10.13427/j.cnki.njyi.2014.08.031.

[11] Li, B., Liu, Y., Niu, G. et al. (2020). Analysis of the Research Dynamics of Straw Crushing and Returning Machine and Key Components (秸秆粉碎还田机及关键部件的研究动态分析). *Agricultural Mechanization in Xinjiang*, No.203 (05): 10-13. https://doi.org/10.13620/j.cnki.issn1007-7782.2020.05.003.

[12] Lian, X. J., Li, J., Wang, H., et al. (2009). Regularity for change of respiration intensity of different sweet potato varieties at normal atmospheric temperature (不同品种甘薯常温贮藏期间呼吸强度变化规律). *Transactions of the Chinese Society of Agricultural Engineering*, 25(6): 310-313. 10.3969/j.issn. https://doi.org/1002-6819.2009.06.058.

[13] Lv, J., Shang, Q., Yang, Y. et al. (2016). Design Optimization and Experiment on Potato Haulm Cutter (马铃薯杀秧机设计优化与试验). *Journal of Agricultural Machinery*, 47(05):106-114+98. https://doi.org/10.6041/ j.issn.1000-1298.2016.05.015.

[14] Mu, G., (2021). Research on the key technology and device of crushing and throwing of sweet potato seedling recycling machine imitating the ridge type (仿垄式甘薯秧回收机粉碎抛送关键技术与装置研究). *Shandong Agricultural University*. https://doi.org/10.27277/d.cnki.gsdnu.2021.000973.

[15] Pan, F., Kang, J., Yan, L. (2015). Design and experiment to key components of Y type cutting device of smashed straw machine (Y 型甩刀式秸秆粉碎还田机关键部件的设计与性能试验). *Research of agricultural modernization*, 36(05):912-915. https://doi.org/10.13872/j.1000-0275.2015.0090.

[16] Phesatcha, K., & Wanapat, M. (2013). Performance of lactating dairy cows fed a diet based on treated rice straw and supplemented with pelleted sweet potato vines. *Tropical animal health and production* (2). https://doi.org/10.1007/s11250-012-0255-5.

[17] Shi, L., Hu, Z., Gu, F. et al. (2017). Sign and parameter optimization on teeth residue plastic film collector of ridged peanut (耙齿式垄作花生残膜回收机设计及参数优化). *Transactions of the Chinese Society of Agricultural Engineering*, 33(02):8-15. https://doi.org/10.11975/j.issn.1002-6819.2017.02.002.

[18] Wang, X., Zhang, M., Mu, T. (2012). Process optimization on alcohol production using sweet potato residue by simultaneous saccharification and fermentation method (甘薯渣同步糖化发酵生产酒精的工艺优化). *Transactions of the Chinese Society of Agricultural Engineering*, 28(14): 256-261. https://doi.org/10.3969/j.issn.1002-6819.2012.14.039.

[19] Wu, F., Xu, H., Gu, F. et al. (2017). Improvement of straw transport device for straw-smashing back-throwing type multi-function no-tillage planter (秸秆粉碎后抛式多功能免耕播种机秸秆输送装置改进). *Transactions of the Chinese Society of Agricultural Engineering*, 33(24):18-26. https://doi.org/10.11975/j.issn.1002-6819.2017.24.003.

[20] Wu, T., Wang, G., Hu, L., et al. (2018). Modal analysis of the knife roller of walking type sweet potato chopper-returning machine (步行式甘薯碎蔓还田机刀辊模态分析). *Journal of Jiangsu Normal University (Natural Science Edition)*, 36(03):47-49+53. https://doi.org/10.3969/j ISSN. 2095-4298.2018.03.009.

[21] Xia, Y., He, Y., Wang, W. et al. (2011). Experimental research on mechanized harvesting pattern of sweet potato in sections (分段红薯机械化收获模式实验研究). *Chinese Agricultural Mechanization*, No.238(06):70-72+69. https://doi.org/10.3969/j.issn.1006-7205. 2011.06.017.

[22] Xie, Y., Bian, X., Jia, Z. et al. (2022). Development status and prospect of fresh sweet potato industry in China (中国鲜食甘薯产业发展现状及其发展前景). *Jiangsu J. of Agr. Sci*, 38(06):1694-1701. https://doi.org/10.3969/j.issn.1000-4440.2022.06.028.

[23] Yan, W., Hu, Z., Wu, N. et al. (2017). Parameter optimization and experiment for plastic film transport mechanism of shovel screen type plastic film residue collector (铲筛式残膜回收机输膜机构参数优化与试验). *Transactions of the Chinese Society of Agricultural Engineering*, 33(01):17-24. https://doi.org/10.11975/j.issn.1002-6819.2017.01.003.

[24] Yu, Z., Hu Z., Wang, H., et al. (2015). Parameter optimization and experiment of garlic picking mechanism (大蒜果秧分离机构参数优化及试验). *Transactions of the Chinese Society of Agricultural Engineering*, 31(01):40-46. https://doi.org/10.3969/j.issn.1002-6819.2015.01.006.

[25] Yuan, B., Xue, L., Zhang, Q., et al. (2016). Essential Oil from Sweet Potato Vines, a Potential New Natural Preservative, and an Antioxidant on Sweet Potato Tubers: Assessment of the Activity and the Constitution. *Journal of agricultural and food chemistry* (40). https://doi.org/10.1021/acs.jafc.6b03175.

[26] Zhang, J., Wang, X., Chen, F. et al. (2007). Design of new multifunctional straw crushing and returning recycling machine (新型多功能秸秆粉碎还田回收机的设计). *Research on agricultural mechanization*, No.150(10):65-67. https://doi.org/10.13427/j.cnki.njyi.2007.10.030.

[27] Zhang, M., Jin, C., Liang, S. et al. (2015). Parameter optimization and experiment on air-screen cleaning device of rapeseed combine harvester (风筛选式油菜联合收割机清选机构参数优化与试验). *Transactions of the Chinese Society of Agricultural Engineering*, 31(24):8-15. https://doi.org/10.11975/j.issn.1002-6819.2015.24.002.

[28] Zhao, Y., Wang, Y., Liu, H. et al. (2018). Design and Test of Stubble-breaking Components on Strip Subsoiling and Stubble-breaking Machine (带状深松灭茬机灭茬部件设计与试验). *Journal of Agricultural Machinery*, 49(03):94-103. https://doi.org/10.6041/j.issn.1000-1298.2018.03.011.